Atmos. Chem. Phys. Discuss., 13, 7061–7079, 2013
www.atmos-chem-phys-discuss.net/13/7061/2013/
doi:10.5194/acpd-13-7061-2013

Atmospheric Chemistry and Physics Discussions

In situ detection of electrified aerosols in the upper troposphere and in the stratosphere

J.-B. Renard[1], S. N. Tripathi[2], M. Michael[2], A. Rawal[2], G. Berthet[1], M. Fullekrug[3], R. G. Harrison[4], C. Robert[1], M. Tagger[1], and B. Gaubicher[1]

[1]LPC2E-CNRS/University of Orléans, UMR7328, 3A avenue de la recherche scientifique, 45071 Orléans cedex 2, France
[2]Indian Institute of Technology, Kanpur, Center for Environmental Science and Engineering, India
[3]University of Bath, Department of Electronic and Electrical Engineering, Claverton Down, Bath, BA2 7AY, UK
[4]University of Reading, Department of Meteorology, Reading RG6 6BB, UK

Received: 16 December 2012 – Accepted: 8 February 2013 – Published: 18 March 2013

Correspondence to: J.-B. Renard (jean-baptiste.renard@cnrs-orleans.fr)

Published by Copernicus Publications on behalf of the European Geosciences Union.

Abstract

Electrified aerosols have been observed in the lower troposphere and in the mesosphere, but have never been detected in the stratosphere and upper troposphere. We present measurements of aerosols during a balloon flight to an altitude of ~ 24 km. The measurements were performed with an improved version of the STAC aerosol counter dedicated to the search for charged aerosols. It is found that most of the aerosols are charged in the upper troposphere for altitudes below 10 km and in the stratosphere for altitudes above 20 km. On the contrary, the aerosols seem to be uncharged between 10 km and 20 km. Model calculations are used to quantify the electrification of the aerosols with a stratospheric aerosol-ion model. The percentages of charged aerosols obtained with model calculations are in excellent agreement with the observations below 10 km and above 20 km. On the other hand, the model cannot reproduce the absence of detected electrification in the lower stratosphere, such that a distinct unknown process in this altitude range inhibits electrification. The presence of sporadic transient layers of electrified aerosol in the upper troposphere and in the stratosphere could have significant implications for sprite formation.

1 Introduction

The main origin and key properties of aerosols in the Earth's atmosphere vary across atmospheric layers. For example, a large variety of natural and anthropogenic particles (e.g., sulphates, soot, minerals etc.) with a complex chemistry (e.g. Tie et al., 2005) are found in the troposphere. In the stratosphere, liquid aerosols originate from gases like carbonyl sulphide (OCS) (Brühl et al., 2012) and sulphur dioxide (SO_2) which is released during volcanoes eruptions (Haywood et al., 2010). For example, the eruption of the Mount Pinatubo in 1991 strongly increased the stratospheric aerosol content for several years (Deshler et al., 2003). Smaller eruptions of volcanoes are more numerous and help to sustain the "background" aerosol content in the stratosphere (Vernier et

ACPD
13, 7061–7079, 2013

al., 2011); these volcanoes are therefore sometimes named “stratovolcanoes”. In addition to these liquid aerosols, solid particles have been detected in the lower and middle stratosphere (Renard et al., 2008; Ciucci et al., 2008; Neely et al., 2011). Stratospheric soot particles mainly originate from biomass burning injected into the stratosphere by pyroconvection (Fromm and Servranckx, 2003). It is speculated that soot particles could also originate from anthropogenic activities (Schwarz et al., 2006). Aerosols from meteoritic debris (e.g. Klekociuk et al., 2005) and interplanetary grains are present at all altitudes, with occasional local and temporal enhancements. Such solid particles could for example explain the sporadic aerosol layer detected above 30 km by Renard et al. (2010). Finally, in the mesosphere, the recondensation of disintegrated meteoritic material produces “smoke particles” (Gabrielli et al., 2004; Amyx et al., 2008; Herving et al., 2009).

Some of these aerosols have electric charges. In disturbed weather in the troposphere, droplets can be charged within thunderstorms and electrified shower clouds, but even in the fair weather atmosphere, aerosol particles charge from ion diffusion (Gunn, 1954; Keefe et al., 1959; Clement and Harrison, 1991). Accordingly we expect a proportion of aerosol particles always to be charged, depending on the local ion concentrations and temperature. Droplet charging at edges of stratiform clouds has been attributed to current flow associated with cosmic ray ionisation (Nicoll and Harrison, 2010). Electric discharges also have been detected in volcanic ashes (Gilbert et al., 1991; Thomas et al., 2007; Harrison et al., 2010) and in Saharan dust layers (Nicoll et al., 2011). These aerosols are electrified under the influence of the natural atmospheric electricity. In the mesosphere, smoke and ice particles are part of the plasma in the D-region and carry positive and negative charges (Hoppe, 1999; Rapp, 2009). Yet, the possible charging of liquid and solid particles in the stratosphere has not been much studied. This paper describes the first in situ measurements of electrified aerosols in the stratosphere, which are compared with theoretical model calculations. The implications of these observations are discussed in the context of the global atmospheric electric circuit.

ACPD
13, 7061–7079, 2013

2 Measurement technique of uncharged and charged aerosols

The in situ measurements of aerosols are obtained by use of the optical Stratospheric and Tropospheric Aerosol Counter (STAC) on board a stratospheric balloon payload (Renard et al., 2008). The STAC instrument measures the light scattered by aerosols that cross a laser beam, one by one, at a scattering angle of 70°. The intensity of scattered light is proportional to aerosol size, and counting of the scattered light pulses provides aerosol concentration in 13 size classes from 0.33 to 5.5 µm. The instrument has been calibrated to observe liquid droplets. In the presence of solid aerosols, the intensity of scattered light is generally smaller than for liquid aerosols. As a result the concentration for a given size class can be underestimated, because the concentration of solid aerosols is attributed to lower size classes (Renard et al., 2010).

In its usual form, STAC cannot distinguish between charged and uncharged aerosols. Therefore we have developed an electric trap to remove charged particles, which is mounted between the air inlet and the optical chamber. The electric trap is based on multiple plate-shaped electrodes spaced at 5 mm distance. Using a difference in potential of 220 V between two consecutive electrodes, a deflecting electric field of 45 $kV\,m^{-1}$ is generated. Particles are pumped through the electric trap under laminar gas-flow conditions, at a flow speed of 33 $mm\,s^{-1}$. For particles of radii from 0.3 µm to a few µm with densities expected for stratospheric aerosols, their deflection time within the electric field is a few microseconds. The trap only allows the uncharged aerosols emerging to enter the optical chamber of the aerosol counter to cross the laser beam. Even so, some charged aerosols may remain despite the trap, for example under unexpected large stratospheric aerosol concentrations. Hence the measurements provide, at least, a lower limit of charged particles concentrations.

During the experiments, two identical STAC instruments were operated in parallel on the same balloon gondola, one with the electric trap to measure the concentration of uncharged aerosols, and one without the trap to measure the total concentration of aerosols. The concentration of charged particles is calculated by subtracting the

ACPD
13, 7061–7079, 2013

counts of the two instruments. This method can determine the concentration of charged aerosols – and therefore the proportion of aerosols charged – but not the polarity of the charge. The comparison of the relative counts from the two STAC instruments is not affected by the presence of solid particles, because the associated bias described above is the same for uncharged and charged particles.

Laboratory tests showed that the electric trap does not introduce a bias. Uncharged solid aerosols were injected in an air volume pumped by the two STAC instruments; they measure the same concentrations of aerosols for all size classes in the 0.3–5 µm range. Same conclusions were obtained for ambient air composed of liquid and solid aerosols.

3 Vertical profiles

A stratospheric balloon carrying the two STAC instruments was launched by the French space agency CNES on 12 March 2011, from Kiruna, Northern Sweden (67°53′ N, 21°04′ E). The balloon flight lasted from 20:00–22:05 UT. The measurements with the STAC instruments were specifically conducted during the ascent in the 480–28 hPa altitude range and during the slow descent in the 28–130 hPa altitude range with the vertical speed in the range of 2–5 $m\,s^{-1}$). Figure 1 shows the measurement of uncharged aerosol concentrations during the measurement process as described above. Similar curves were obtained during the descent. The flight was performed during typical conditions of aerosol content, i.e. with concentrations of the smallest particles decreasing with altitude and a maximum concentration around the tropopause (located here around the ~ 300 hPa level, corresponding to an altitude of ~ 8 km). The change of the concentration envelopes for aerosols greater than 1 µm in comparison with smaller sizes is expected to be an indicator of the presence of solid particles. This more or less constant concentration of large solid particles has been observed in previous flights (Renard et al., 2010).

ACPD
13, 7061–7079, 2013

The measured concentrations are subsequently summarised in three size classes: 0.35–1 µm, 1–3 µm, > 3 µm, because the aerosol concentrations are relatively low, especially for micron aerosol. Figure 2 presents the vertical profiles of concentrations for all aerosols and for uncharged aerosols in these 3 size classes (left), and the percentage of charged aerosols (right). It is noted that the measurements during the ascent and the descent are in excellent agreement with respect to the concentrations for both uncharged and charged aerosols. The three size classes exhibit the same dependence on altitude: most of the aerosols (∼ 90 %) are charged in the upper troposphere for altitudes up to 10 km (pressure > 200 hPa) and in the middle stratosphere for altitudes down 20 km (pressure < 50 hPa). Furthermore, the proportion charged is greater for the larger particles sizes, as expected from thermodynamic considerations (Keefe et al., 1959). In contrast, the aerosols seem to be uncharged in the layer between the tropopause and the middle stratosphere, i.e., between ∼ 8.5 km to ∼ 20 km during this flight.

4 Model

Model calculations are used to quantify the electrification of the aerosols with a stratospheric ion-aerosol model in the altitude range from 5–24 km. This is on the assumption of diffusion charging from the ions formed by background cosmic ray ionisation (Harrison and Carslaw, 2003). The ionisation is greatest between 14 and 17 km. This ion pair production rate is calculated using the statistical model of O'Brien (2005). The major ions considered here are SO_4^{2-} and NH_4^+. Electrons are not included in the model as they recombine with positive ions and uncharged molecules very rapidly and are not available to interact with aerosols. The charging of aerosols is calculated using charge balance equations as described in Michael et al. (2008, 2009) and Tripathi et al. (2008). Equations (1) and (2) show the rate of change of +ve (n^+) and –ve (n^-) ion concentrations, which depend on ion pair production rate (q), ion-ion recombination coefficient (α), aerosol concentration (S), and ion-aerosol attachment rate (β).

ACPD
13, 7061–7079, 2013

$$\frac{dn^+}{dt} = q - \alpha n^+ n^- - \left[n^+ \sum_{j=r_1}^{r_{end}} \sum_{i=-m}^{m} \beta_{ij}^+ S_{ij} \right] \quad (1)$$

$$\frac{dn^-}{dt} = q - \alpha n^+ n^- - \left[n^- \sum_{j=r_1}^{r_{end}} \sum_{i=-m}^{m} \beta_{ij}^- S_{ij} \right] \quad (2)$$

Here the radii of the aerosols vary from size r_1 to r_{end} and the maximum charge an aerosol can possess is "m". The aerosol concentration for any size and charge is calculated by Eq. (3), where i represents the charge on aerosol and j represents the radius bin.

$$\frac{dS_{ij}}{dt} = \beta_{i-1,j}^+ S_{i-1,j} n^+ + \beta_{i+1,j}^- S_{i+1,j} n^- - \beta_{i,j}^+ S_{i,j} n^+ - \beta_{i,j}^- S_{i,j} n^- \quad (3)$$

The ion-aerosol attachment coefficients are computed using the method of Hoppel and Frick (1986) and the ionic mobility and mean free path are calculated using the expression from Borucki et al. (1982).

A polydisperse distribution of aerosols is used in the model, which are obtained from the STAC measurements of the total aerosol concentration. The neutral atmospheric properties like temperature and pressure measured during the flight are used in the model. For each size category considered in the polydisperse aerosol, a maximum of $m = \pm 20$ unit electronic charges are considered on each of the particles. The charge balance equations are solved by a fourth order Runge-Kutta numerical method, and the concentrations of positive ions, negative ions, uncharged aerosols and charged aerosols are obtained at the steady state.

Figure 3 presents the initial and final ion concentrations from the simulation. As the initial concentrations of positive and negative ions are the same, only positive ion concentrations are shown in the figure. These ions are removed by the ion-aerosol attachment; it is shown that this ion removal is very small for altitudes less than 8 km.

ACPD
13, 7061–7079, 2013

For the rest of the atmosphere, about 5–10 % of the ions are removed by ion-aerosol interactions.

The conductivity of the atmosphere is a function of the concentration of the ions and their mobilities, and is calculated by Eq. 4):

$$\sigma = e\left(n_{+}K_{+} + n_{-}K_{-}\right) \tag{4}$$

where e is the electronic charge, n_{+} and n_{-} are the number densities and K_{+} and K_{-} are the mobilities of positive and negative ions respectively. About 5–10 % of the ions are removed by the ion-aerosol interactions, thus decreasing the conductivity of the atmosphere.

Figure 4a shows the simulated probability of charge distribution on particles at 8 km in the atmosphere. Particles with radii 0.33–1 µm can carry only a few charges (i.e. only less than 1 % of the particles can carry charges more than ±4) and about 20 % of the particles remain neutral. Only 11 % of the particles in the size range 1–3.3 µm remain uncharged and less than 1 % of the particles can carry more than ±7 electronic charge. Bigger particles (radius > 3.3 µm) show a more flat distribution and carry up to ±10 electronic charges. The ion-aerosol attachment coefficients increases as the size of the particles and therefore larger particles carry more charges compared to the smaller particles (Tripathi et al., 2008; Michael et al., 2008, 2009). Figure 4b and c show similar results, but for altitudes 15 km and 21 km in the atmosphere.

According to Fig. 5, the concentration of neutral particles shows a good agreement between the model and the observation below 10 km and above 20 km. In the lower stratosphere, the model and the observations are inconsistent. The observations indicate that most of the particles remain neutral while the simulations show that about 90 % of the particles are charged. Hence we could speculate that a process not represented in the model inhibits electrification in this altitude range. Such a process would have to act to remove the ions present, or greatly increase their mobility, slowing the diffusion charging. It might be associated with the vertical transport and mixing of air

ACPD
13, 7061–7079, 2013

masses, but we cannot totally exclude the possibility of an unknown instrumental artefact.

5 Discussion and conclusion

Even though it is currently not possible to determine the exact nature of the aerosols, the novel results strongly underpin the need for more detailed measurements and modelling. For example, the electric properties of aerosols could depend on their shape, i.e., liquid droplets have a smaller surface area than fractal-shaped particles like soot. It is expected that liquid aerosols are associated with sub-micron sizes and solid particles are associated with larger sizes. Yet, the aerosol is likely to be much more complex because of the presence of soot particles in the submicron and micron size range, thereby increasing the complexity of future modelling work.

The presence of sporadic transient layers of electrified aerosols in the middle stratosphere could have significant implications for sprite formation. Sprites are transient streamer discharges in the atmosphere above thunderclouds (Franz et al., 1990; Sentman et al., 1995). They are caused by impact ionization resulting from the electromagnetic fields associated with intense positive lightning discharges (e.g. Boccippio et al., 1995; Pasko, 2010). The key parameter to explain sprite initiation is the charge moment change resulting from the lightning continuing current (Cummer and Stanley, 1999; Cummer and Fullekrug, 2001). The threshold for sprite initiation varies by at least a factor of ~ 2 or more which may be explained by nocturnal mesospheric conductivity variations (Cummer and Lyons, 2005), intra-cloud lightning discharges (Ohkubo et al., 2005), or possibly meteoritic dust (Zabotin and Wright, 2001). In either case, it is commonly believed that positive lightning discharges with continuing current are a necessary, but not necessarily sufficient condition to initiate sprites. The possible presence of sporadic transient layers of electrified aerosols in the middle stratosphere reported in this contribution may result in a significant enhancement of the electric field in the middle stratosphere which reaches up to the stratopause and beyond into the mesosphere

ACPD
13, 7061–7079, 2013

and could thereby assist sprite initiation. This hypothesis clearly warrants testing by flying a balloon above or nearby sprite producing thunderstorms to measure the electrified aerosol content with aerosol counters equipped to detect charged aerosols.

Thus, flights of the new Light Optical Aerosol Counter (LOAC) will be performed in near future in different geophysical conditions, to better document the altitude profile of the electrified aerosols.

Acknowledgements. The AEROWAVE project is funded by CNES and CNRS/INSU. The work at the University of Bath is supported by the Natural Environment Research Council (NERC) under grant NE/H024921/1. The modelling work at IIT, Kanpur is supported by Ministry of Earth Sciences, India. We thank the CNES balloon launching team for the STAC flight. We thank Jean-Pierre Lebreton (LPC2E-CNRS) for their fruitful comments. Stratospheric aerosols data and other balloon measurements on stratospheric species are available on the ETHER website: http://ether.ipsl.jussieu.fr/.

The publication of this article is financed by CNRS-INSU.

References

Amyx, K., Sternovsky, Z., Knappmiller, S., Robertson, S., Horanyi, M., and Gumbel, J.: In-situ measurement of smoke particles in the wintertime polar mesosphere between 80 and 85 km altitude, J. Atmos. Solar-Terr. Phys., 70, 61–70, doi:10.1016/j.jastp.2007.09.013, 2008.

Boccippio, D. J., Williams, E. R., Heckman, S. J., Lyons, W. A., Baker, I., and Boldi, R.: Sprites, ELF Transients and Positive Ground Strokes, Science, 269, 1088–1091, doi:10.1126/science.269.5227.1088, 1995.

ACPD
13, 7061–7079, 2013

Borucki, W. J., Levin, Z., Whitten, R. C. , Keesee, R. G., Capone, L. A.,, Toon, O. B., and Dubach, J. Predicted electrical conductivity between 0 and 80 km in the Venusian atmosphere, Icarus, 51, 302–321, 1982.

Brühl, C., Lelieveld, J., Crutzen, P. J., and Tost, H.: The role of carbonyl sulphide as a source of stratospheric sulphate aerosol and its impact on climate, Atmos. Chem. Phys., 12, 1239–1253, doi:10.5194/acp-12-1239-2012, 2012.

Clement, C. F. and Harrison, R. G., Charge distributions on aerosols, Institute of Physics Conference Series, 118, 275–280, 1991.

Ciucci, A., Palumbo, P., Brunetto, R., Della Corte,V., De Angelis , S., Rotundi, A., Rietmeijer, F. J. M., Zona, E., Colangeli, L., Esposito, F., Mazzotta Epifani, E., Mennella, V., Inarta, S., Peterzen, S., Masi, S., and Ibba, R.: DUSTER (Dust in Upper Stratosphere Tracking Experiment and Retrieval) preliminary analysis, Mem. S. A. It., 75, 282–287, 2008.

Cummer, S. A. and Füllekrug, M.: Unusually intense continuing current in lightning produces delayed mesospheric breakdown, Geophys. Res. Lett., 28, 495–498, 2001.

Cummer, S. A. and Lyons, W. A.: Implications of lightning charge moment changes for sprite initiation, J. Geophys. Res., 110, A04304, doi:10.1029/2004JA010812, 2005.

Cummer, S. A. and Stanley, M.: Submillisecond resolution lightning currents and sprite development: Observations and implications, Geophys. Res. Lett., 26, 3205, doi:10.1029/1999GL003635, 1999.

Deshler, T., Hervig, M. E., Hofmann, D. J., Rosen, J. M., and Liley, J. B.: Thirty years of in situ stratospheric aerosol size distribution measurements from Laramie, Wyoming (41° N) using balloon-borne instruments J. Geophys. Res., 108, 4167, doi:10.1029/2002JD002514, 2003.

Franz, R. C., Nemzek R. J., and Winckler, J. R.: Television Image of a Large upward Electric Discharge above a Thunderstorm System, Science, 249, 48–51, doi:10.1126/science.249.4964.48, 1990.

Fromm, M. and Servranckx, R.: Transport of forest fire smoke above the tropopause by supercell convection, Geophys. Res. Lett., 30, 1542, doi:10.1029/2002GL016820, 2003.

Gabrielli, P., Barbante, C., Plane, J. M., Varga, A., Hong, S., Cozzi, G., Gaspari, V., Planchon, F. A., Cairns, W., Ferrari, C., Crutzen, P., Cescon, P., and Boutron, C. F.: Meteoric smoke fallout over the Holocene epoch revealed by iridium and platinum in Greenland ice, Nature, 432, 1011–1014, doi:10.1038/nature03137, 2004.

Gilbert, J. S., Lane, S. J., Sparks, R. S. J., and Koyaguchi, T.: Charge measurements on particle fallout from a volcanic plume, Nature, 349, 598–600, 1991.

ACPD
13, 7061–7079, 2013

Gunn, R.: Diffusion charging of atmospheric droplets by ions, and the resulting combination coefficients, J. Meteorol., 11, 339–347, 1954.
Harrison, R. G. and Carslaw, K. S.: Ion-aerosol-cloud processes in the lower atmosphere, Rev. Geophys., 41, 1012, doi:10.1029/2002RG000114, 2003.
Harrison, R. G., Nicoll, K. A., Ulanowski, Z., and Mather, T. A.: Self-charging of the Eyjafjallajökull volcanic ash plume, Environ. Res. Lett., 5, 024004, doi:10.1088/1748-9326/5/2/024004, 2010.
Haywood, J. M. et al.: Observations of the eruption of the Sarychev volcano and simulations using the HadGEM2 climate model, J. Geophys. Res., 115, D21212, doi:10.1029/2010JD014447, 2010.
Hervig, M. E, Gordley, L. L., Deaver L. E., Siskind D. E., Stevens, M. H., Russell III, J. M., Bailey, S. M., Megner L., and Bardeen, C. G: First Satellite Observations of Meteoritic Smoke in the Middle Atmosphere, Geophys. Res. Lett., 36, L18805, doi:10.1029/2009GL039737, 2009.
Hoppe, U.-P., Eriksen, T., Thrane, E., Blix, T. A., Fiedler, J., and Lübken, F.-J.: Observations in the polar middle atmosphere by rocket-borne Rayleigh lidar: First results, Earth Planets Space, 51, 815–824, 1999.
Hoppel, W. A. and Frick, G. M.: Ion-aerosol attachment coefficients and the steady-state charge on aerosols in a bipolar ion environment, Aerosol Sci. Technol., 5, 1–21, 1986.
Keefe, D., Nolan, P. J., and Rich, T. A.: Charge equilibrium in aerosols according to the Boltzmann law, Proc. R. Irish Acad., 60A, 27–45, 1959.
Klekociuk, A., Brown, P. G., Pack, D. W., ReVelle, D. O., Edwards, W. N., Spalding, R. E., Tagliaferri, E., Yoo, B. B., and Zagari, J.: Meteoritic dust from the atmospheric disintegration of a large meteoroid, Nature, 436, 1132–1135, doi:10.1038/nature03881, 2005.
Michael, M., Triapthi, S. N., and Mishra, S. K.: Dust charging and electrical conductivity in the day and nighttime atmosphere of Mars, J. Geophys. Res., 113, E07010, doi:10.1029/2007JE003047, 2008.
Michael, M., Tripathi, S. N., Borucki, W. J., and Whitten, R. C.: Highly charged cloud particles in the atmosphere of Venus, J. Geophys. Res., 114, E04008, doi:10.1029/2008JE003258, 2009.
Neely, R. R., English, J. M., Toon, O. B., Solomon, S., Mills, M., and Thayer, J. P.: Implications of extinction due to meteoritic smoke in the upper stratosphere, Geophys. Res. Lett., 38, L24808, doi:10.1029/2011GL049865, 2001.

ACPD
13, 7061–7079, 2013

Nicoll, K. A. and Harrison R. G.: Experimental determination of layer cloud edge charging from cosmic ray ionization, Geophys. Res. Lett., 37, L13802, doi:10.1029/2010GL043605, 2010.
Nicoll, K. A., Harrison, R. G., and Ulanoswki, Z.: Observations of Saharan dust layer electrification, Environ. Res. Lett., 6, 014001, doi:10.1088/1748-9326/6/1/014001, 2011.
O'Brien, K.: The theory of cosmic-ray and high-energy solar particle transport in the atmosphere, The natural radiation environment VII, edited by: McLaughlin, J. P., Simopoulos, S. E., and Steinhusler, F., Elsevier, Amsterdam, 2005.
Ohkubo, A., Fukunishi, H., Takahashi, Y., and Adachi, T.: VLF/ELF sferic evidence for in-cloud discharge activity producing sprites, Geophys. Res. Lett., 32, L04812, doi:10.1029/2004GL021943, 2005.
Pasko, V. P.: Recent advances in theory of transient luminous events, J. Geophys. Res., 115, A00E35, doi:10.1029/2009JA014860, 2010.
Rapp, M.: Charging of mesospheric aerosol particles: the role of photodetachment and photoionization from meteoric smoke and ice particles, Ann. Geophys., 27, 2417–2422, doi:10.5194/angeo-27-2417-2009, 2009.
Renard, J.-B., Brogniez, C., Berthet, G., Bourgeois, Q., Gaubicher, B., Chartier, M. Balois, J.-Y., Verwaerde, C., Auriol, F., Francois, P., Daugeron, D., and Engrand, C.: Vertical distribution of the different types of aerosols in the stratosphere, detection of solid particles and analysis of their spatial variability, J. Geophys. Res., 113, D21303, doi:10.1029/2008JD010150, 2008.
Renard, J.-B., Berthet, G., Salazar, V., Catoire, V., Tagger, M., Gaubicher, B., and Robert, C.: In situ detection of aerosol layers in the middle stratosphere, Geophys. Res. Lett., 37, L20803, doi:10.1029/2010GL044307, 2010.
Schwarz, J. P., Gao, R. S., Fahey, D. W., Thomson, D. S., Watts, L. A., Wilson, J. C., Reeves, J. M., Darbeheshti, M., Baumgardner, D. G., Kok, G. L., Chung, S. H., Schulz, M., Hendricks, J., Lauer, A., Kärcher, B., Slowik, J. G., Rosenlof, K. H., Thompson, T. L., Langford, A. O., Loewenstein, M., and Aikin, K. C.: Single-particle measurements of mid-latitude black carbon and light-scattering aerosols from the boundary layer to the lower stratosphere, J. Geophys. Res., 111, D16207, doi:10.1029/2006JD007076, 2006.
Sentman, D. D., Wescott, E. M., Osborne, D. L., Hampton, D. L., and Heavner M. J.: Preliminary results from the Sprites94 Aircraft Campaign: 1. Red sprites, Geophys. Res. Lett., 22, 1205–1208, doi:10.1029/95GL00583, 1995.

ACPD
13, 7061–7079, 2013

Tie, X., Madronich, S., Walters, S., Edwards, D. P., Ginoux, P., Mahowald, N., Zhang, R. Y., Lou, C., and Brasseur, G.: Assessment on the global impact of aerosols on tropospheric oxidants, J. Geophys. Res., 110, doi:10.1029/2004JD005359, 2005.

Tripathi, S. N., Michael, M., and Harrison, R. G.: Profiles of Ion and Aerosol Interactions in Planetary Atmospheres, Space Sci. Rev., 30, 193–211, doi:10.1007/s11214-008-9367-7, 2008.

Vernier, J.-P., Thomason, L. W., Pommereau, J.-P., Bourassa, A., Pelon, J., Garnier, A., Hauchecorne, A., Blanot, L., Trepte, C., Degenstein, D., and Vargas, F.: Major influence of tropical volcanic eruptions on the stratosphere aerosol layer during the last decade, Geophys. Res. Lett., 38, L12807, doi:10.1029/2011GL047563, 2011.

Zabotin, N. A. and Wright, J. W.: Role of meteoric dust in sprite formation, Geophys. Res. Lett., 28, 2593–2596, doi:10.1029/2000GL012699, 2011.

ACPD
13, 7061–7079, 2013

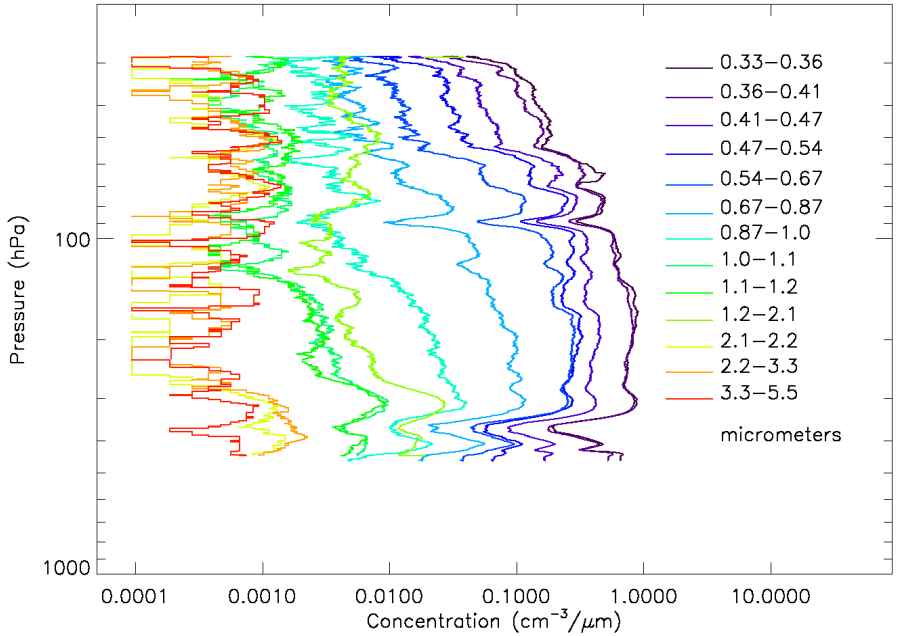

Fig. 1. Vertical profiles of the charged and uncharged aerosol concentration, on 12 March 2011 from Kiruna (Northern Sweden) during the balloon ascent.

ACPD
13, 7061–7079, 2013

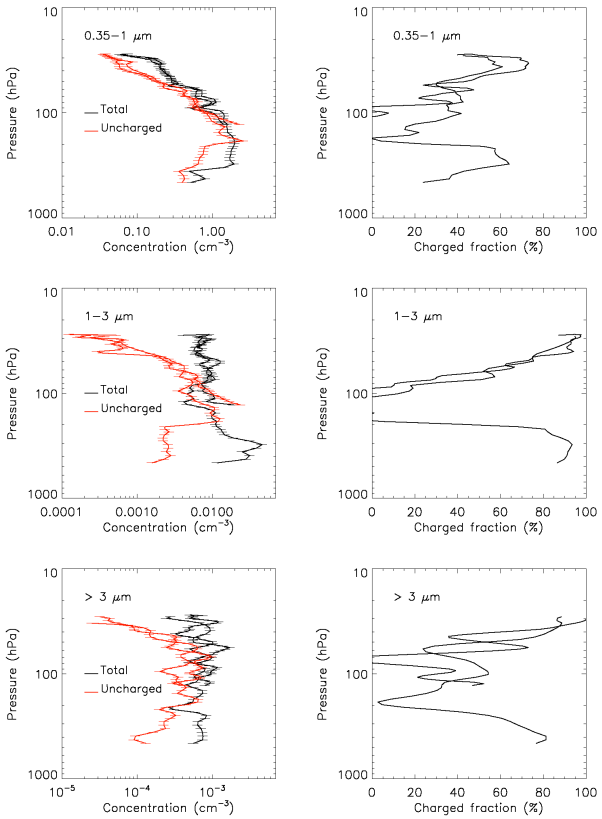

Fig. 2. Left, vertical profiles of integrated concentrations for all the aerosols ("total") and for the charged aerosols, during the balloon ascent and the descent, for the 3 size classes; right, percentage of charges aerosols for the 3 size classes (a sliding smoothing is applied to suppress small length-scale fluctuations).

ACPD
13, 7061–7079, 2013

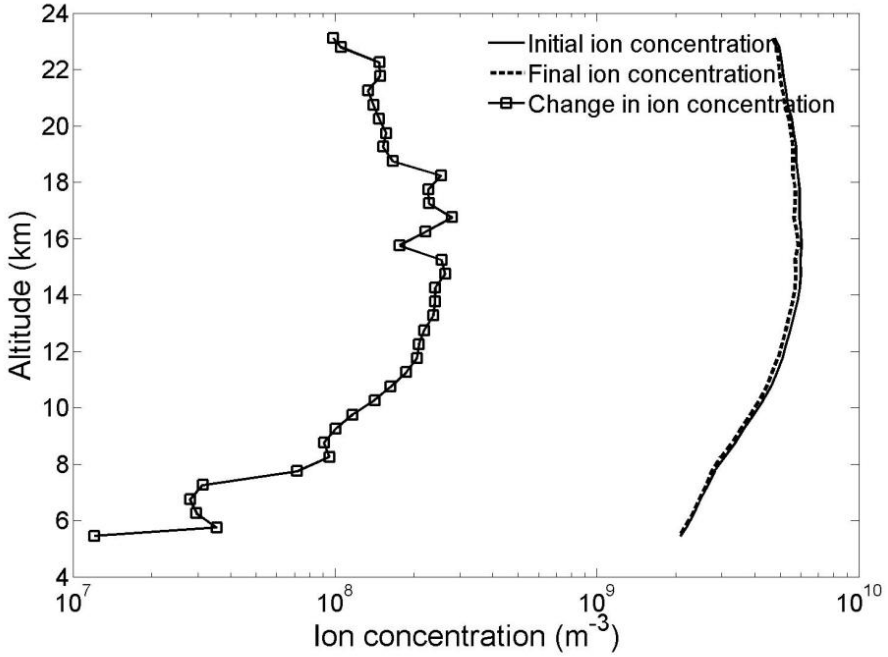

Fig. 3. The initial and final ion concentrations from modelling calculations.

ACPD
13, 7061–7079, 2013

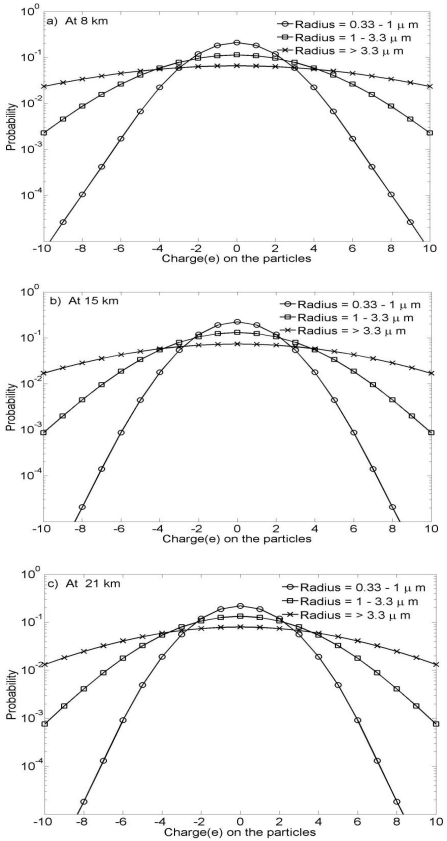

Fig. 4. Probability of charge distribution on aerosols at **(a)** 8 km, **(b)** 15 km, **(c)** 21 km, from modelling calculations.

ACPD
13, 7061–7079, 2013

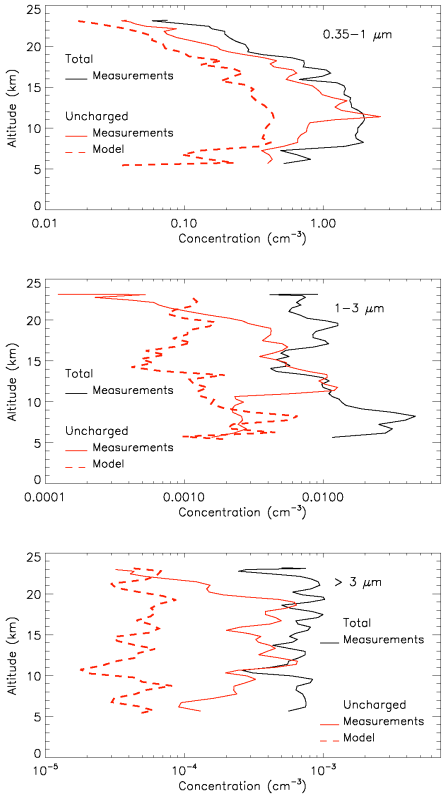

Fig. 5. Comparison between measurements (solid lines) and modelling (dashed lines). The Figure shows the data collected during the ascent which exhibit a standard deviation of ∼ 15 % (not shown). The altitude scale is given in km for comparison with the altitude scale in Figs. 1 and 2 given in hPa. The modelling data are constrained by the total concentration of aerosols measured by STAC.

ACPD
13, 7061–7079, 2013